Unraveling the Meaning of Effective Uptake Coefficients in Multiphase and Aerosol Chemistry

Ryan Reynolds[1,2] and Kevin R. Wilson[1,*]

[1] *Chemical Sciences Division, Lawrence Berkeley National Laboratory, Berkeley CA 94720*
[2] *Department of Chemistry, University of California, Berkeley, CA 94720*

Conspectus:

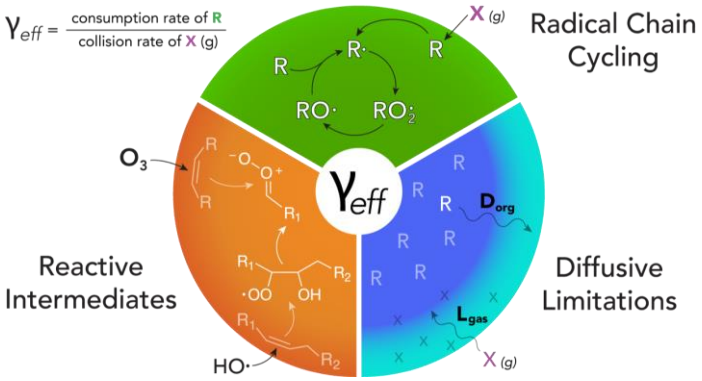

Reactions of gas phase molecules with surfaces play key roles in atmospheric and environmental chemistry. Reactive uptake coefficients (γ), the fraction of gas-surface collisions that yield a reaction, are used to quantify the kinetics in these heterogeneous and multiphase systems. Unlike rate coefficients for homogeneous gas or liquid phase reactions, uptake coefficients are emergent quantities that depend upon a multitude of underlying elementary steps. As such, uptake coefficients adopt complex scaling behavior with reactant concentrations and other physicochemical properties of the interface, making predictions of γ particularly challenging.

Typically, γ_{gas} is obtained by measuring the loss rate of a gas phase molecule above a liquid or solid surface relative to its collision frequency. By definition, $\gamma_{gas} \leq 1$. Highly efficient reactions proceed at or near the gas-surface collision frequency and exhibit values of γ_{gas} near unity. Alternatively, heterogeneous kinetics are often measured using the consumption rate of a condensed phase reactant normalized to the gas-surface collision frequency, yielding instead an effective uptake coefficient (γ_{eff}). In many cases, γ_{eff} and γ_{gas} are not equal, yielding additional insights into the nature of the reaction. For example, substantial diffusive limitations in the condensed phase may inhibit reactivity, yielding $\gamma_{eff} << \gamma_{gas}$. In contrast, $\gamma_{eff} > \gamma_{gas}$ in the presence of condensed phase secondary reactions, with values of γ_{eff} often exceeding 1 for the case of radical chain reactions.

In this account, we will discuss how measurements of γ_{eff} in aerosol reveal the origins of complex physical and chemical behavior in multiphase reactions that can be uniquely observed and understood through the lens of effective uptake coefficients. For example, the scaling of γ_{eff} with water vapor in aqueous systems, or shell thickness in core-shell aerosol, yields insight into relative transport and reaction timescales of gaseous oxidants, while the scaling of γ_{eff} with oxidant and trace gas concentrations provides a distinctive signature of the underlying competition between

free radical propagation and termination mechanisms. Further, changes in γ_{eff} induced by careful selection of the molecular structure of the condensed-phase reactants help identify new reaction pathways and indirectly report on the reaction kinetics of short-lived species, including Criegee Intermediates. Through these examples we will show how proper experimental design and accurate measurements of an effective uptake coefficient can be used to interrogate complex multiphase reaction mechanisms.

Key References

- Davies, J. F.; Wilson, K. R. Nanoscale Interfacial Gradients Formed by the Reactive Uptake of OH Radicals onto Viscous Aerosol Surfaces. *Chem. Sci.* **2015**, *6* (12), 7020–7027. *Utilizes the nonlinear dependence of the effective uptake coefficient with relative humidity to quantify changes in reacto-diffusive length in viscous aerosols.*

- Richards-Henderson, N. K.; Goldstein, A. H.; Wilson, K. R. Large Enhancement in the Heterogeneous Oxidation Rate of Organic Aerosols by Hydroxyl Radicals in the Presence of Nitric Oxide. *J. Phys. Chem. Lett.* **2015**, *6* (22), 4451–4455. *Effective uptake coefficients are shown to increase with the availability of NO, which initiates alkoxy-radical secondary chemistry.*

- Zeng, M.; Heine, N.; Wilson, K. R. Evidence That Criegee Intermediates Drive Autoxidation in Unsaturated Lipids. *PNAS* **2020**. *Decreases in effective uptake coefficients with the addition of scavenger molecules show that Criegee intermediates are formed during radical-initiated lipid autoxidation.*

- Reynolds, R.; Ahmed, M.; Wilson, K. R. Constraining the Reaction Rate of Criegee Intermediates with Carboxylic Acids during the Multiphase Ozonolysis of Aerosolized Alkenes. *ACS Earth Space Chem.* **2023**. *Uses effective uptake coefficients to monitor the rates of Criegee Intermediate-scavenging reactions and radical chain cycling chemistry.*

Introduction

Multiphase reactions are often quantified in terms of a reactive uptake coefficient (γ). γ is defined as the net loss of gas-phase molecules entering the condensed phase, divided by their collision rate with the surface.[1,2] This definition developed in the context of reactions on aqueous interfaces, *e.g.* cloud droplets in the atmosphere, by expanding on notions of mass accommodation coefficients (α).[3,4] Measuring γ can be straightforward for many reaction systems, such as by use of a Knudsen cell or coated flow tube, given that it only requires monitoring relative changes in the flux of gas and not absolute concentrations,[1] and thus can account for the effects of evaporation, desorption, diffusion, and reaction.[5]

However, interpreting the physical meaning of γ has been shown to be an increasing challenge over several decades of measurement and analysis. For aerosol reactions, simple frameworks, such as the resistor model,[4] which assumes that the particle is well-mixed and all processes contributing to gas uptake are independent, often break down when applied to systems where reaction and diffusion are strongly coupled.[6,7] As attention in aerosol research has shifted toward particles of primarily organic constituents, such descriptions of the kinetics have been stretched to the edges of their useful working ranges[8] for organic aerosols with semisolid and highly viscous phase states, in which high concentrations and slow mixing of reactants prove troublesome for analysis in terms of limiting kinetic cases.[9,10] Additionally, for reactions involving gas-phase radicals, γ is often hard to measure, as radical concentrations are generally low, difficult to detect, and can induce significant amounts of chemistry in the particle phase that is not directly reflected in gas-phase measurements.

Alternately, heterogeneous reactions on aerosols with primarily organic constituents can be described in terms of the *effective* uptake coefficient, γ_{eff}, defined as the consumption rate of a condensed-phase reactant relative to the collision rate of the impinging gas (Figure 1).[11] In such a measurement (typically by an aerosol mass spectrometer), the collision rate of a trace gas with the particle surface is used as a clock against which the reaction time can be measured. For an aerosol with an arbitrary condensed-phase reactant R undergoing reaction with a gas X, γ_{eff} is defined in terms of the loss of R,

$$\frac{d[R]}{dt} = -k_{R-X}[R][X] = -\gamma_{X,eff}^{R} \cdot (C_p \cdot A) \cdot f \cdot J_{coll,X} \qquad \text{Eq. (1)}$$

where $k_{R\text{-}X}$ is the phenomenological 2nd-order rate constant for the reaction of R with X, C_p and A are the number concentration of the aerosol and surface area of a single aerosol particle, respectively. f is the fraction of R remaining in the aerosol at any point during the reaction, and $J_{coll,X}$ is the flux of X onto the particle surface,

$$J_{coll,X} = \frac{\bar{c}[X]}{4} \qquad \text{Eq. (2)}$$

where $\bar{c}$ is the mean molecular speed of X. For single-component well-mixed spherical particles this expression reduces to,

$$\gamma_{X,eff}^{R} = \frac{4k_{R-X}D_{surf}\rho_0 N_A}{6\bar{c}M_R} \qquad \text{Eq. (3)}$$

with D_{surf} the surface-weighted particle diameter, ρ_0 the density of R, M_R its molar mass, and N_A Avogadro's number.

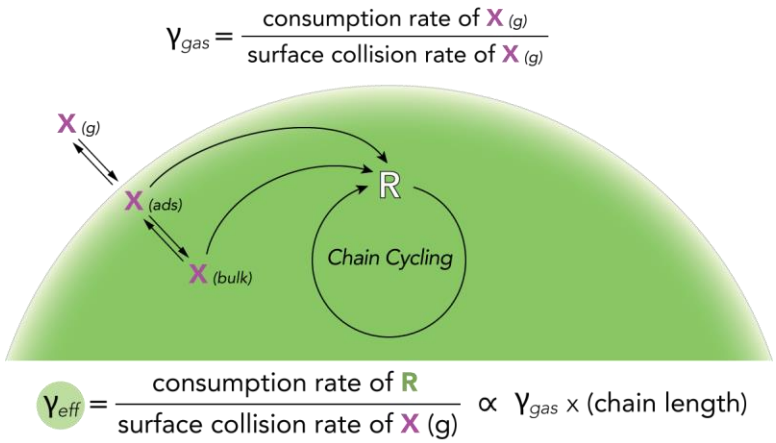

Figure 1. Schematic illustrating the effects of chain cycling chemistry on the measurement of γ_{gas} and γ_{eff}.

Since γ_{eff} is measured from the perspective of the condensed phase reactant, it is often not equivalent to the uptake coefficient measured from the gas phase (γ_{gas}, Figure 1). For example, in the presence of diffusive limitations, which inhibit reaction, $\gamma_{eff} \ll \gamma_{gas}$, or when secondary reactions in the condensed phase provide additional sinks for reactants, $\gamma_{eff} > \gamma_{gas}$, potentially exceeding unity, such as in the case of radical chain reactions with long chain lengths. γ_{gas}, in contrast, cannot exceed 1 by definition. Thus, γ_{eff} is an emergent property of each reaction system, and through careful measurement and interpretation can be used to interrogate multiple facets of a multiphase reaction mechanism.

In the following Account, we will discuss the versatility of γ_{eff} as an experimental observable by examining its role in our group's studies of model organic aerosols under laboratory conditions (*e.g.*, in flow tube reactors). These measurements under controlled conditions demonstrate how γ_{eff} can report on diffusion coefficients and the timescales of reactant mixing in semisolid aerosol,[12–14] elucidate competitions between radical propagation and termination mechanisms in chemical reactions,[11,15–17] and help identify new chemical mechanisms involving

short-lived reactive intermediates.[18–20] We conclude by discussing how information gained from measurements of γ_{eff} can be applied to the chemistry of atmospheric particles and other systems of interest.

Insights Into the Relative Timescales of Transport and Reaction

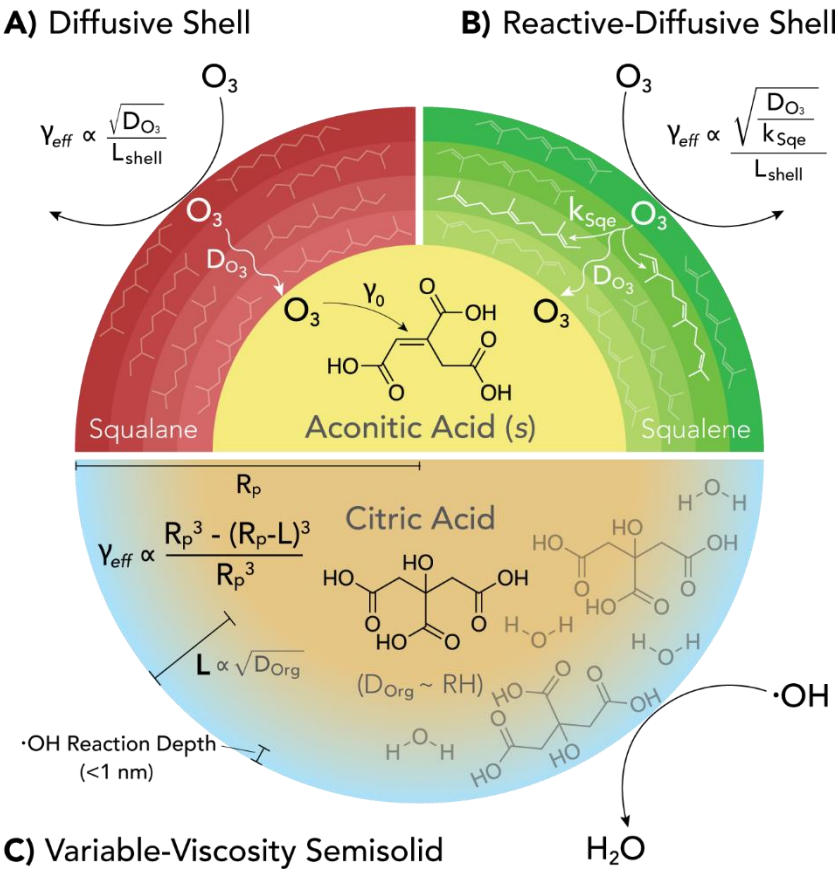

Figure 2. Schematic illustrating the relationship between γ_{eff} and reactant transport in ozone reactions with core-shell particles having (a) diffusive and (b) reactive-diffusive organic shells, and (c) in OH radical reactions with citric acid (CA) particles of varying viscosity.

Organic aerosols in the atmosphere can exist in a wide variety of phase states, with particle viscosities ranging from liquid to semisolid (tar-like) and solids,[10,21–23] and recent studies have emphasized how phase state can determine both the transport of gaseous reactants into aerosol particles and the mixing behavior of the particle constituents themselves. Determining the

characteristic length- and timescales that govern transport and mixing can be experimentally challenging, especially when these processes are inextricably linked with particle-phase chemical reactions. However, given proper experimental technique, measurements of γ_{eff} can be used to quantify key transport parameters in aerosol particles.

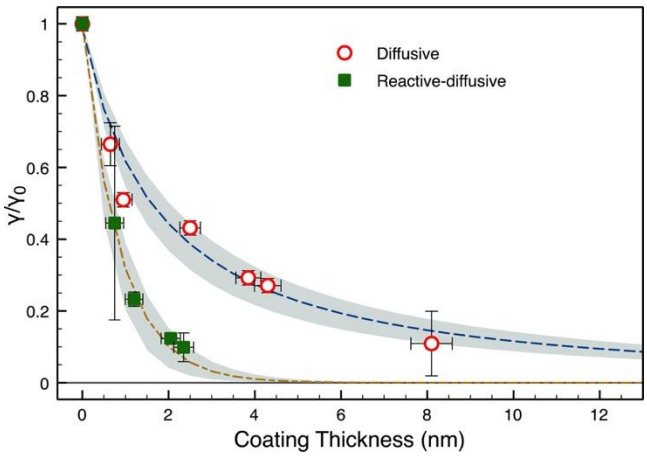

Figure 3. The scaling of γ_{eff} with the thickness of purely diffusive and reactive-diffusive shells in model core-shell aerosol upon ozone exposure. Reprinted with permission from Lee *et al.*[12]. Copyright 2016 American Chemical Society.

One such technique was demonstrated by Lee *et al.,*[12] who generated core-shell aerosols with cores of *trans*-aconitic acid (an unsaturated tricarboxylic acid, Figure 2) that react with a known rate ($\gamma_{eff} = \gamma_0$) upon exposure to ozone (O_3). The reactive cores were coated with a thin layer of lipid-like, liquid organic, creating a phase-separated shell whose thickness could be determined within ±1 nm by particle size measurements. Depending on whether the shell was a saturated hydrocarbon (Squalane (Sqa), $C_{30}H_{62}$) or an unsaturated hydrocarbon (Squalene (Sqe), $C_{30}H_{50}$), an O_3 molecule colliding with the particle surface would be subject to either diffusion (Figure 2A) or both diffusion and reaction (Figure 2B) as it transits through the shell, increasing the time required to reach and react with the core. As the shell thickness was increased from 0 up

to 12 nm, γ_{eff} for the aconitic acid core was observed to decrease, and the barrier coefficient (the ratio of γ_{eff} to the γ_0 of the uncoated core) was plotted as a function of coating thickness (Figure 3).

Since the particle morphology and coating thicknesses were known, each set of barrier coefficients in Figure 3 could be fit using a single parameter related to the transport of O_3 through the shell. In the case of aerosol with purely diffusive shells (Figure 2A), the decrease in γ_{eff} is directly related to the diffusion coefficient, D_{O_3}, of ozone in Squalane, with a value of D_{O_3} = $1.6\text{x}10^{-6}$ cm^2 s^{-1} estimated by fitting. However, in the case of reactive-diffusive shells (Figure 2B), the transit time through the shell additionally depends on the chemical lifetime of O_3 in Squalene, estimated by $\tau_{rxn} = 1/k_{Sqe}[Sqe]_0$. The relative effects of both diffusion and reaction can be expressed as one parameter, the reacto-diffusive length $L_{O_3} = \sqrt{D_{O_3}\tau_{rxn}}$. This length is the average distance an O_3 molecule diffuses in the shell before reacting with an Sqe molecule, with the fitted value of L = 1.03 nm corresponding roughly to the *e*-folding thickness of the barrier coefficient in Figure 3. Additionally, by assuming that the value of D_{O_3} is the same for both shell types, the chemical lifetime of O_3 in Sqe was found to be on the order of 7 ns. Thus, by analyzing how γ_{eff} is modulated, the transport properties of a gaseous reactant could be investigated even when reaction and diffusion are coupled.

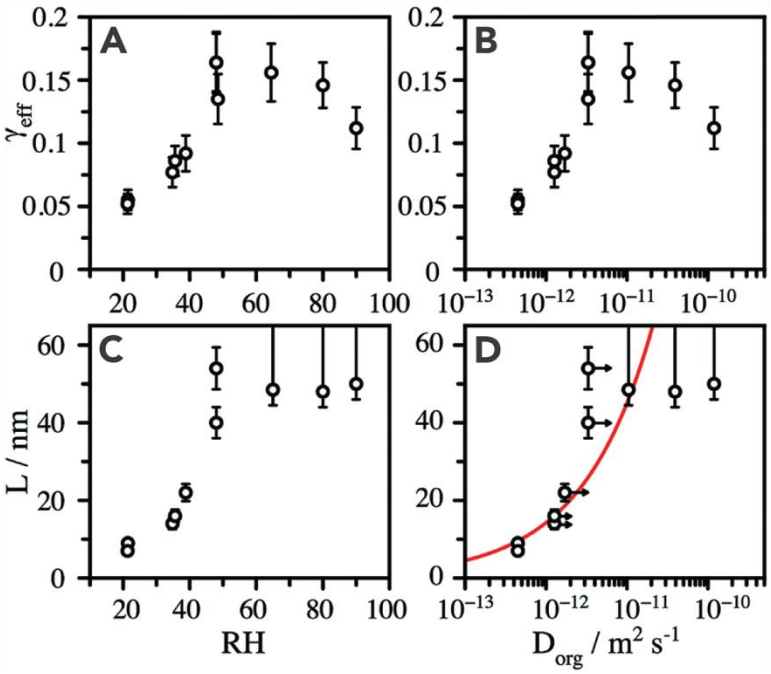

Figure 4. Scaling of γ_{eff} (panels A–B) and the accessible depth L (panels C–D) with citric acid + OH radical oxidation (panels A-D). Adapted from Davies *et al.*[13] with permission from the PCCP Owner Societies.

While this phase-separated system proved useful for controlled experiments, another challenge lies in understanding how reactivity changes when the particle phase state is in a transitional regime, for example beginning in a solid or semi-solid state and becoming more liquid-like.[6,7,13] Davies *et al.* explored such a transition by reacting submicron citric acid (CA) aerosol with gas-phase hydroxyl radicals (OH) in a flow tube reactor (Figure 2C).[13] CA is a hygroscopic, amorphous solid whose viscosity depends on the relative humidity (RH): below 50% RH, CA is a diffusion-limited semi-solid, while at 50% RH and above, CA aerosols behave like well-mixed aqueous solutions. From the known viscosity at each RH, a self-diffusion coefficient of CA (D_{org}) can be estimated using the Stokes-Einstein relation.

The decay kinetics of CA upon OH exposure were then monitored using mass spectrometry. γ_{eff} was calculated under each set of conditions, showing an expected dependence on RH (Figure 4A), and therefore on D_{org} (Figure 4B): below 50% RH, γ_{eff} increases with

increasing diffusion rates, reaching an inflection point at 50% RH. Beyond 50% RH, the dilution effect of added water leads to a decrease in uptake. However, the reacto-diffusive length of OH in the CA aerosol yields is calculated to be less than 1 nm over all values of D_{org}, indicating that the reaction takes place primarily at the particle surface. Surface-sensitive measurements supported this conclusion, as the reaction kinetics in the near-surface region appeared well-mixed at all RH values, while whole-particle measurements indicated a fraction of the aerosol remained unreacted below 50% RH.

These results are explained using an accessible-volume model, which relates γ_{eff} to the reaction depth, L (Figure 2C), which is the depth of a surface shell of the particle in which the CA appears well-mixed on the timescale of OH reaction. By fitting this model to the observed values of γ_{eff}, values of L can be found as a function of RH (Figure 4C). Similar to a reacto-diffusive length, L is roughly proportional to the square root of D_{org} (red line, Figure 4D) until L exceeds the particle radius (R_p) and the entire particle is well-mixed and available for reaction. However, instead of the transport of the gas-phase reactant limiting the reaction as with core-shell aerosols, it is the timescale of CA diffusion in the particle phase, which controls its ability to replenish the surface region and therefore controls value of γ_{eff}. These experiments nicely illustrate how γ_{eff} encodes information about the transport timescales of not only incoming gas-phase reactants, but also the subsurface mixing time of particle phase reactants.

In addition to directly modulating the uptake, varying transport times can also have indirect effects on the reactivity in complex reactions. Houle *et al.*[14] conducted detailed reaction-diffusion simulations of the OH oxidation of hydrocarbons under various diffusion limitations and showed that characteristic length scales can exist for individual particle-phase reaction steps. When diffusive limitations restrict the mobility of particle-phase reactants to within these characteristic

lengths, changes can occur in the reaction mechanism. While further work is still needed to extend these methods to the complex behavior observed in atmospheric organic aerosol, measurements of γ_{eff} can provide mechanistic insight into how transport and reaction are coupled together across phases.

Insights into Competing Mechanisms During Radical Reactions

We turn now to a more explicit treatment of the relationship between γ_{eff} and chemistry in the particle phase, where reactions between free radicals and organic molecules often involve complex mechanisms with many competing processes (Scheme 1). After the reaction is initiated by an incoming radical abstracting a hydrogen atom from a C–H bond (Reaction R1), the reaction can either propagate, by forming new radical species that are in turn capable of H-abstraction, or terminate through radical-radical recombination reactions. To understand the behavior of these radical mechanisms under a variety of conditions, one must inquire as to the key steps and species responsible for propagating the radical chain chemistry, as well as the major reactions which compete with each of these steps. Measurements of γ_{eff} are uniquely suited to address these questions since values of $\gamma_{eff} > 1$ are clear signatures of radical chain chemistry. Thus, by examining how γ_{eff} scales with the concentrations of key reactants, crucial mechanistic steps can be inferred.

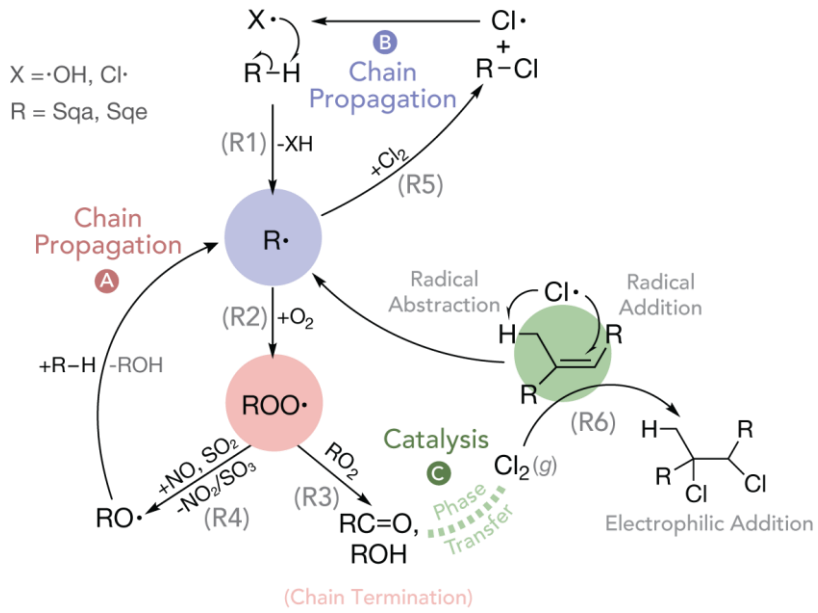

Scheme 1. Summary of the radical-initiated reaction pathways discussed in this section. The "resources" at the heart of the key kinetic competition in each example are highlighted and color-coded.

For example, Richards-Henderson *et al.* examined reactions of OH radicals with aerosols composed of alkanes, particularly Sqa.[15,16] Under atmospheric conditions, where molecular oxygen (O_2) is abundant, once an alkyl radical R· is formed (R1) it quickly reacts with O_2 to produce a peroxy radical, (RO_2, reaction R2).[24] Hydrogen abstraction by RO_2 is relatively slow, so under most laboratory conditions (where radical densities are high), recombination reactions are favored (e.g., RO_2 + RO_2). Recombination yields either chain terminating products (aldehydes, ketones, and alcohols—reaction R3), or alkoxy (RO) radicals, which in turn can propagate the reaction.[25–27] In the particle phase, however, the RO-formation channel does not appear as competitive with chain-terminating recombination, so that an OH reaction with an alkane aerosol under pristine conditions does not exhibit chain cycling ($\gamma_{eff} \leq 1$).[28,29]

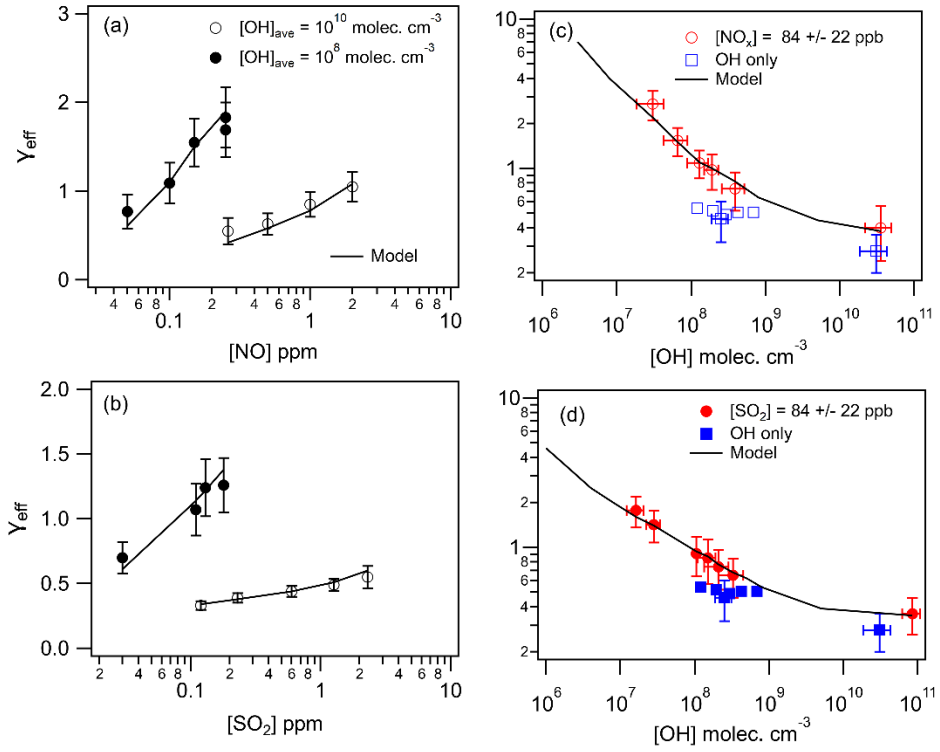

Figure 5. Scaling behavior of γ_{eff} during OH radical-initiated oxidation of Squalane in the presence of trace NO (a, c) and SO_2 (b, d). Adapted with permission from Richards-Henderson, *et al.*[15,16]. Copyright 2016 American Chemical Society.

However, when OH radical oxidation is conducted in the presence of NO and SO_2 (Figure 5), $\gamma_{eff} > 1$, signaling the onset of radical chain cycling. As seen in Figure 5A–B, γ_{eff} scales directly with the concentration of the trace gas, since both NO and SO_2 can undergo oxidation by RO_2 to yield an RO radical (reaction R4, Scheme 1), which propagates the reaction *via* hydrogen abstraction (Label A, Scheme 1). Additionally, for each trace gas, γ_{eff} exhibits an inverse dependence on the radical concentration [OH], with increased reaction probabilities at low concentrations. At high [OH], the increased production of RO_2 radicals favors chain termination (R3), since the recombination rate scales as $[RO_2]^2$, effectively out-competing RO formation (R4). Conversely, at low [OH], the reaction between RO_2 and NO/SO_2 dominates the kinetics, leading to RO radicals and subsequent chain cycling. These results demonstrated that, in the presence of

SO_2 and NO, the lifetimes of alkanes in atmospheric aerosol could be equivalent to or shorter than the corresponding gas-phase lifetimes. Thus, measurements of γ_{eff} helped identify mechanisms by which particle phase chemistry in polluted conditions could accelerate atmospheric aging.

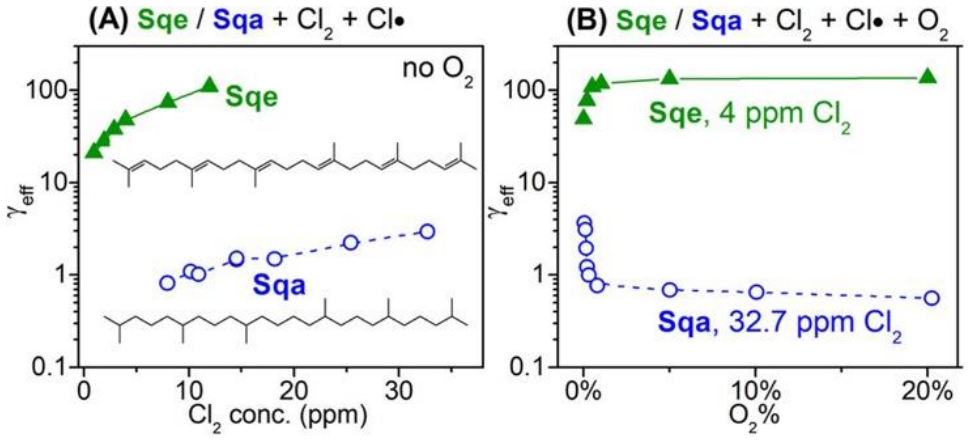

Figure 6. Scaling of γ_{eff} with (A) [Cl_2] in the absence of oxygen and (B) [O_2] at constant Cl_2 concentration for the Cl-initiated reaction of Squalane (Sqa) and Squalene (Sqe). Adapted with permission from Zeng *et al.*[30]. Copyright 2022 American Chemical Society.

In addition to OH oxidation, Liu *et al.* studied the reaction of chlorine gas with aerosols of the same saturated hydrocarbon (Sqa).[11] In these experiments, highly reactive chlorine atoms (Cl·) are produced by photolyzing molecular chlorine (Cl_2), and thus both species are present during reaction. As with OH, the reaction is initiated by abstraction of a hydrogen from a C–H bond of Sqa (R1), but in the absence of atmospheric oxygen (O_2), the reaction exhibits $\gamma_{eff} \geq 1$, indicating chain cycling (Figure 6A, blue open circles). While Cl_2 is unreactive towards saturated hydrocarbons, increases in Cl_2 concentration lead to an increase in γ_{eff} under these anoxic conditions, as the reaction between Cl_2 and an alkyl radical R· regenerates a Cl· (Reaction R5, Scheme 1), which can initiate hydrogen abstraction and propagate the chain reaction (Label B, Scheme 1). By comparing the values of γ_{eff} to the primary uptake coefficient (*i.e.*, γ_{gas}) inferred

from kinetic modeling, it was estimated that an upper bound of 6 Sqa molecules were consumed by secondary reactions for each reactive collision of gas phase Cl·.[11]

When O_2 is reintroduced, however, the chain-propagating step (R5) must compete with the formation of RO_2 radicals (R2).[11] When [O_2] is at atmosphere concentrations (~20%), it is orders of magnitude more abundant than either Cl_2 or Cl· in the experiment, leading to high RO_2 concentrations. Again, since the recombination rate scales as $[RO_2]^2$, this leads to the formation of oxygenated products and termination of the radical chain (R3). Therefore, the presence of O_2 shuts down reaction, giving rise to the inverse relationship of [O_2] and γ_{eff} (Figure 6B, blue open circles). Thus, by analyzing the scaling of γ_{eff} with the concentrations of key reactants (O_2 and Cl_2), a rational mechanism for the complex kinetic behavior could be formulated.

However, simple changes in the functional groups available for reaction in the condensed phase can lead to unexpected changes in the reaction mechanism and drastic increases in reactivity, as seen in the chlorination of Sqe aerosols studied by Zeng *et al.*[17] The structure of Sqe is nearly identical to that of Sqa, except for 6 alkene functional groups (C=C bonds), which allows electrophilic addition of Cl_2 to the molecule (Reaction R6, Scheme 1). While this reaction is quite slow for pure Sqe aerosols, the presence of particle-phase additives containing oxygenated functional groups enhanced the effective Cl_2 addition rate by 12-23 times over γ_{gas}.[31] While the precise mechanism of this acceleration is under investigation, it was hypothesized that the oxygenated molecules act as phase transfer catalysts by increasing the Cl_2 residence time at the particle surface.

As a result, when Sqe aerosols were reacted with Cl· in the presence of Cl_2, the combination of Cl_2 electrophilic addition chemistry and the radical cycling mechanism described previously led to an extremely rapid reaction, with γ_{eff} for Sqe (green triangles, Figure 6A) that is roughly two

orders of magnitude larger than for Sqa. But surprisingly, when [O_2] was increased the reaction was accelerated (green triangles, Figure 6B), displaying the opposite the trend in γ_{eff} than that measured previously for Sqa. In addition, the reaction products under high [O_2] were almost entirely chlorinated, not the oxygenated products characteristic of RO_2 recombination and chain termination (R3).

The magnitude of the increase in γ_{eff} therefore eliminates Cl· chain propagation as the source of the accelerated reactivity, as the rate of R5 would not be expected to change so dramatically between Sqa and Sqe. Instead, a catalytic mechanism promoting Cl_2 electrophilic addition chemistry (R6) was proposed.[30] Despite the rapid reaction between Sqe and Cl_2, the radical mechanism described previously is still operative in the presence of high [O_2], leading to RO_2 recombination (R3) and chain termination products. However, these termination products contain the same functional groups as the additives previously observed to catalyze Cl_2 electrophilic addition.[31] Thus, increased [O_2] increases the abundance of these products by generating a Cl_2 phase-transfer catalyst *in situ* in the aerosol (Label C, Scheme 1), which explains the unexpected and dramatic increase of γ_{eff} with [O_2] shown in Figure 6B.

As before, investigation of the behavior of γ_{eff} provided insights into a previously unknown process with significant impacts beyond atmospheric chemistry, such as in heterogeneous catalysis. The observation of catalytic behavior during electrophilic addition chemistry raises new questions to be investigated regarding the role of particle interface in controlling these reaction dynamics. The usefulness of γ_{eff} as a probe for discovering novel reaction mechanisms thus extends beyond radical chemistry, as explored further in the following section.

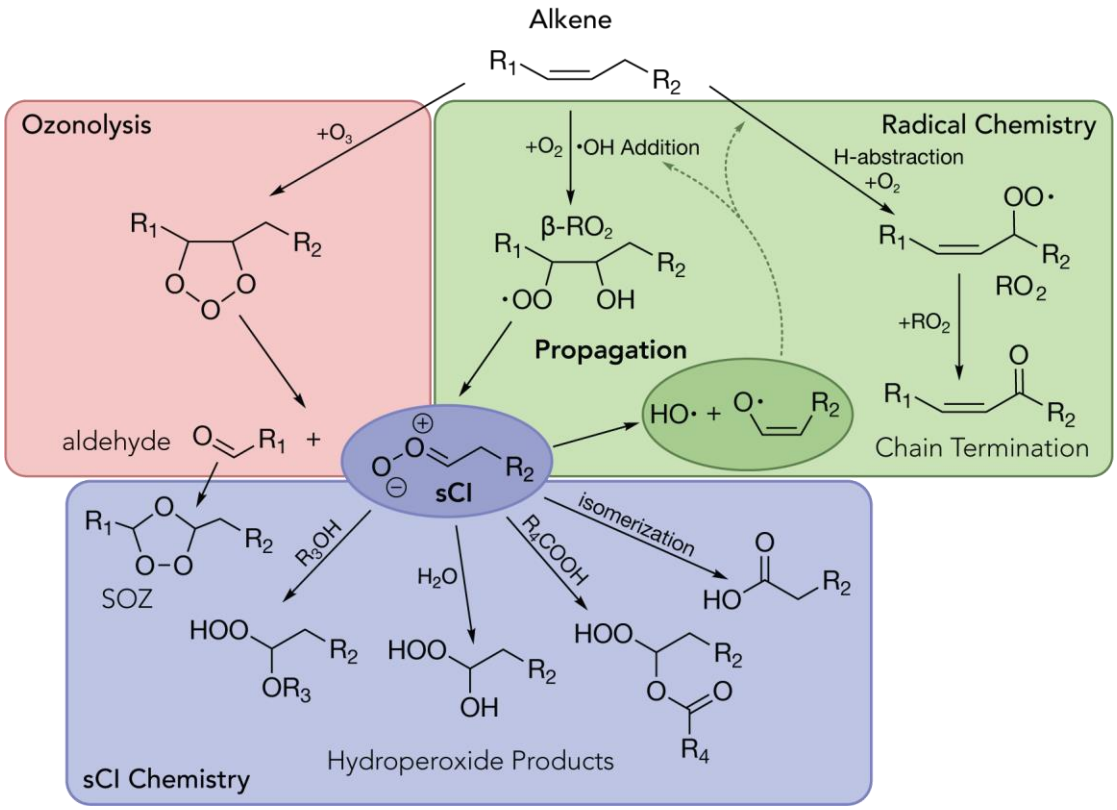

Scheme 2. The interconnected reaction pathways of ozone, free radicals, and stabilized Criegee Intermediates (sCI). Adapted with permission from Zeng *et al.*[19]. Copyright 2020 American Chemical Society.

In addition to examining the scaling behavior of γ_{eff} with gas-phase reactants, modifying the structure of particle-phase reactants can also help elucidate complex reaction mechanisms. One example is the peroxidation of unsaturated lipids, which typically proceeds *via* abstraction of a labile allylic hydrogen adjacent to a C=C bond, followed by addition of O_2 to form an unsaturated RO_2 radical (Scheme 2). Although slow, these species can perform intramolecular hydrogen abstraction from another allylic site, yielding a hydroperoxide (ROOH) and regenerating a R· radical, which propagates the chemistry (known as autoxidation or lipid peroxidation).[32] However,

experiments on lipid oxidation have traditionally been performed in the bulk condensed phase using radical initiators, instead of realistic radical species such as OH.[33,32]

To probe this reaction mechanism in aerosols, radical oxidation experiments were again conducted on aerosols of Sqe, a common component of human skin oil, with oxidation initiated by OH.[18] The scaling of γ_{eff} with [OH] shows increased chain cycling at low oxidant concentrations (Figure 7). The unsaturated sites play a role in the mechanism, as decreasing the number of C=C bonds in the particle phase reactant from 6 (Sqe) to 1 (*cis*-9-tricosene, Tri) leads to a decrease in γ_{eff}. By contrast, saturated molecules with a single oxygenated functional group all have $\gamma_{eff} < 1$, indicating the absence of chain cycling.

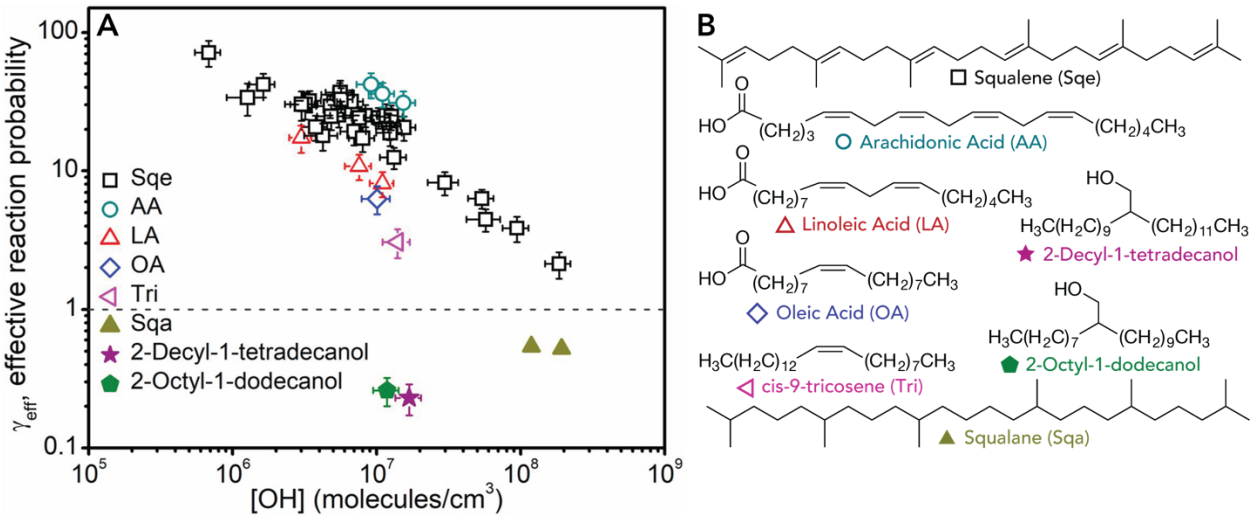

Figure 7. (a) Scaling of γ_{eff} with [OH] for various particle-phase organics shown in (b), both unsaturated (Sqe, AA, LA, OA, and Tri) and saturated (Sqa, 2-Decyl-1-tetradecanol, 2-Octyl-1-dodecanol). Figure adapted with permission from Zeng *et al.*[18] Copyright 2020 National Academy of Sciences

These kinetics could be interpreted as consistent with a typical lipid peroxidation mechanism, however upon analysis, the reaction products were found not to be hydroperoxides

(ROOH), but rather secondary ozonides (SOZs), which are typically only observed during ozonolysis (Scheme 2).[34] These species form from the reaction of aldehydes and stabilized Criegee Intermediates (sCI, not to be confused with Chlorine/Cl·), which are highly reactive molecules formed during ozonolysis. As first shown by Beauchamp and coworkers,[35] sCIs appear to be formed during radical-initiated oxidation of unsaturated lipids. To test this hypothesis, saturated alcohols, which can act as sCI scavengers, were incorporated into the particle phase with Sqe.[18] The result was the formation of characteristic sCI + alcohol hydroperoxide ether products (Scheme 2), a gradual decrease in the γ_{eff} of Sqe as alcohol was added, and a drastic enhancement in the γ_{eff} of the alcohol above its value in pure droplets (Figure 8A). These results imply that sCIs are not only generated during OH oxidation, but are in fact the species responsible for its chain propagation, as sCIs can regenerate OH radicals *via* unimolecular decomposition channels.

The precise mechanism by which sCIs are produced remains under investigation, though several mechanisms have been proposed[18,35–37] each involving the β-hydroxy peroxy radical (β-RO_2) formed after OH addition to the alkene (Scheme 2). A recent modeling study of the OH oxidation of Sqe evaluated the kinetic viability of 3 possible mechanisms,[38] but further combined theoretical and experimental efforts are needed to establish a comprehensive description of this step.

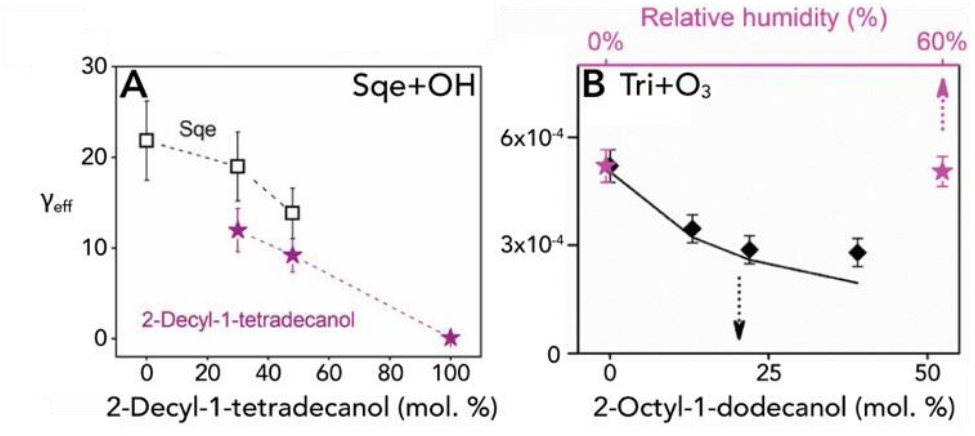

Figure 8. Scaling of γ_{eff} with the concentration of sCI scavenger (saturated alcohol) in the condensed phase during (a) OH-radical initiated Sqe oxidation. (Figure adapted with permission from Zeng *et al.*[18] Copyright 2020 National Academy of Sciences) and (b) ozonolysis of Tri aerosol (Figure adapted with permission from Zeng and Wilson.[19] Copyright 2020 American Chemical Society.) The value of γ_{eff} is corrected for the mole fraction of the reactant in these mixture experiments to account for dilution effects.

Regardless of the specific mechanism by which they are generated, sCIs have been shown to constitute a new link between two typically distinct chemical mechanisms, namely secondary chemistry resulting from ozonolysis and OH-initiated radical oxidation (Scheme 2). As a result, radical chain cycling can be initiated by ozonolysis in addition to OH oxidation, as further explored by Zeng *et al.* using *cis*-9-tricosene (Tri) aerosols.[19] Tri has a single C=C bond, which simplifies the reaction mechanism and potential products of ozonolysis, and it has no oxygenated functional groups, which act as sCI scavengers. Additionally, the aldehydes formed from ozonolysis of Tri are volatile and preferentially evaporate from the particle, thereby removing another potential sink of the CI in the particle phase. These properties make Tri an excellent candidate for observing CI-propagated chain cycling.

During ozonolysis, the γ_{eff} of Tri during was measured to be 5.2×10^{-4}, which is an order of magnitude larger than previous measurements of $\gamma_{gas,O3}$.[39] Even though the γ_{eff} is less than 1, substantial chain cycling can still be inferred by comparison of these two measurements. Incorporating a particle-phase saturated alcohol, which is unreactive toward O_3, resulted in the decrease of γ_{eff} (Figure 8B), as was observed for the OH + Sqe reaction (Figure 8A). In addition, a decrease in the radical chain termination products of Tri (Scheme 2) was observed in the presence of alcohol. Surprisingly, kinetic modeling suggests that radical chain cycling is the dominant oxidation pathway for Tri during ozonolysis, accounting for nearly 70% of the reactivity.[19] Thus, this pathway could be kinetically quite significant during ozonolysis chemistry.

However, assessing the significance of this radical chain cycling to atmospheric aerosol aging requires knowledge of the precise rate constants of reactions between sCIs and the various functional groups, such as carboxylic acids, that might be present in these environments.[40] In particular, gas-phase measurements of reactions between small sCIs and carboxylic acids yield a rate constant (k_{acid}) with values at or exceeding the limit for collision-controlled processes,[41,42] but the applicability of this rate to particle-phase sCI is in need of evaluation.

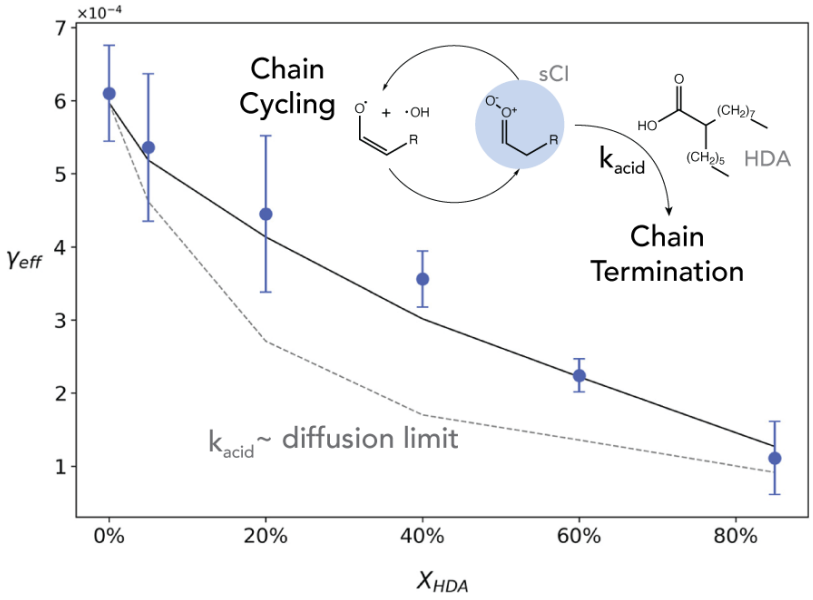

Figure 9. Scaling of γ_{eff} for Tri during ozonolysis as a function of mole fraction of acid sCI scavenger (HDA). Lines correspond to model predictions with differing values of k_{acid}: a slower rate competitive with unimolecular processes (solid line) and the diffusion-limited rate analogous to the collision limit in the gas phase (dashed line). Figure adapted with permission from Reynolds *et al.*[20]. Copyright 2023 American Chemical Society.

Building on previous ozonolysis studies with Tri, an experimental approach involving aerosol mixtures allows the value of k_{acid} in the particle phase to be constrained.[20] Varying amounts of a saturated liquid carboxylic acid, 2-hexyldecanoic acid (HDA), are incorporated into Tri aerosols undergoing ozonolysis where, similar to the behavior with saturated alcohols, the γ_{eff} of Tri decreased. Since HDA is unreactive toward O_3, any decay of HDA observed during ozonolysis

is attributable to sCI chemistry, primarily resulting in a hydroperoxide ester product (Scheme 2). These decay kinetics can be explained in terms of a simple model of the competition between bimolecular reaction of sCIs with HDA, which is chain-terminating, and the unimolecular decomposition reactions of sCIs to initiate radical chemistry, as shown in Figure 9.[20] By fitting this model to the HDA decay profiles observed during Tri ozonolysis, a relative ratio of these rate constants could be obtained. However, measurements of γ_{eff} also constrain the value of the rate constant k_{acid} in kinetic simulations. If the sCI + HDA reaction is extremely fast, it would be expected to proceed at the diffusion limit in the condensed phase, but simulations corresponding to this rate shut off the radical chain cycling too quickly. This leads to a rapid falloff in γ_{eff} with HDA concentration (dashed line, Figure 9) that is inconsistent with experimental observations. Thus, an upper bound can be established on k_{acid}, suggesting a more reasonable rate that keeps this reaction channel competitive with the unimolecular reactions of sCIs.

Through careful experimental design, including changes to the particle-phase composition and molecular structure of the reactants, measurements of γ_{eff} can be used to establish new links between different branches of oxidation chemistry. Applications of this approach thus extend beyond their typical application to heterogeneous reactions on atmospheric aerosols and into research fields such as oxidative stress in biological systems or the design of antioxidants for reducing food spoilage.[18]

Summary and Conclusions

Studies designed around the measurement and interpretation of γ_{eff} have the potential to help explain the complex behavior of chemical systems controlled by reaction and diffusion. By examining the relationship between γ_{eff} and reactant transport parameters, insight is gained into the effects of diffusion limitations on heterogeneous oxidation. By examining the relationship

between γ_{eff} and various gas-phase reactants, the mechanisms of radical reactions can be determined. And by measuring γ_{eff}, while selectively modifying the constituents of the particle phase, new links between disparate reaction mechanisms can be uncovered. We hope it is evident through the examples shown here that the insights gained from these studies have broad applicability both in the field of heterogeneous chemistry and beyond. There are many possible reaction parameters to be explored using γ_{eff} besides those explored in the examples presented here, including studies of γ_{eff} as a function of surface area (*e.g.*, particle size in aerosols) and ambient temperature, which can provide a molecular-level understanding of interfacial processes and reaction thermodynamics. Fundamental insights such as these are crucial to unraveling the behavior of any complex chemical system, from atmospheric aerosols to cellular membranes.

Biographies

Ryan S. Reynolds received his B.A. in Chemistry from Biola University in 2019 and is currently a graduate student at the University of California, Berkeley and Lawrence Berkeley National Laboratory. His research focuses on understanding the role of reactive intermediates in multiphase reaction kinetics using aerosol mass spectrometry techniques.

Kevin R. Wilson is a Senior Scientist in the Chemical Sciences Division of Lawrence Berkeley National Laboratory. He received a B.A. in Chemistry from Willamette University, a M.A. in Liberal Studies from St. John's College and a Ph.D. from the University of California Berkeley. Wilson's research is aimed at understanding the mechanism of multiphase reactions in droplets and aerosols.

Acknowledgements: This work was supported by the Gas Phase Chemical Physics Program (GPCP), in the Chemical Sciences Geosciences and Biosciences Division of the Office of Basic Energy Sciences of the U.S. Department of Energy under Contract No. DE-AC02-05CH11231.

References

(1) Finlayson-Pitts, B. J.; Pitts, J. N. *Chemistry of the Upper and Lower Atmosphere: Theory, Experiments, and Applications*; Academic Press: San Diego, 2000.

(2) Seinfeld, J. H.; Pandis, S. N. *Atmospheric Chemistry and Physics: From Air Pollution to Climate Change*, Third edition.; Wiley: Hoboken, New Jersey, 2016.

(3) Worsnop, D. R.; Zahniser, M. S.; Kolb, C. E.; Gardner, J. A.; Watson, L. R.; Van Doren, J. M.; Jayne, J. T.; Davidovits, P. The Temperature Dependence of Mass Accommodation of Sulfur Dioxide and Hydrogen Peroxide on Aqueous Surfaces. *J. Phys. Chem.* **1989**, *93* (3), 1159–1172. https://doi.org/10.1021/j100340a027.

(4) Davidovits, P.; Kolb, C. E.; Williams, L. R.; Jayne, J. T.; Worsnop, D. R. Mass Accommodation and Chemical Reactions at Gas−Liquid Interfaces. 32.

(5) Kolb, C. E.; Cox, R. A.; Abbatt, J. P. D.; Ammann, M.; Davis, E. J.; Donaldson, D. J.; Garrett, B. C.; George, C.; Griffiths, P. T.; Hanson, D. R.; Kulmala, M.; McFiggans, G.; Pöschl, U.; Riipinen, I.; Rossi, M. J.; Rudich, Y.; Wagner, P. E.; Winkler, P. M.; Worsnop, D. R.; O' Dowd, C. D. An Overview of Current Issues in the Uptake of Atmospheric Trace Gases by Aerosols and Clouds. *Atmos. Chem. Phys.* **2010**, *10* (21), 10561–10605. https://doi.org/10.5194/acp-10-10561-2010.

(6) Berkemeier, T.; Huisman, A. J.; Ammann, M.; Shiraiwa, M.; Koop, T.; Pöschl, U. Kinetic Regimes and Limiting Cases of Gas Uptake and Heterogeneous Reactions in Atmospheric Aerosols and Clouds: A General Classification Scheme. *Atmos. Chem. Phys.* **2013**, *13* (14), 6663–6686. https://doi.org/10.5194/acp-13-6663-2013.

(7) Steimer, S. S.; Berkemeier, T.; Gilgen, A.; Krieger, U. K.; Peter, T.; Shiraiwa, M.; Ammann, M. Shikimic Acid Ozonolysis Kinetics of the Transition from Liquid Aqueous Solution to Highly Viscous Glass. *Phys. Chem. Chem. Phys.* **2015**, *17* (46), 31101–31109. https://doi.org/10.1039/C5CP04544D.

(8) Jimenez, J. L.; Canagaratna, M. R.; Donahue, N. M.; Prevot, A. S. H.; Zhang, Q.; Kroll, J. H.; DeCarlo, P. F.; Allan, J. D.; Coe, H.; Ng, N. L.; Aiken, A. C.; Docherty, K. S.; Ulbrich, I. M.; Grieshop, A. P.; Robinson, A. L.; Duplissy, J.; Smith, J. D.; Wilson, K. R.; Lanz, V. A.; Hueglin, C.; Sun, Y. L.; Tian, J.; Laaksonen, A.; Raatikainen, T.; Rautiainen, J.; Vaattovaara, P.; Ehn, M.; Kulmala, M.; Tomlinson, J. M.; Collins, D. R.; Cubison, M. J.; E; Dunlea, J.; Huffman, J. A.; Onasch, T. B.; Alfarra, M. R.; Williams, P. I.; Bower, K.; Kondo, Y.; Schneider, J.; Drewnick, F.; Borrmann, S.; Weimer, S.; Demerjian, K.; Salcedo, D.; Cottrell, L.; Griffin, R.; Takami, A.; Miyoshi, T.; Hatakeyama, S.; Shimono, A.; Sun, J. Y.; Zhang, Y. M.; Dzepina, K.; Kimmel, J. R.; Sueper, D.; Jayne, J. T.; Herndon, S. C.; Trimborn, A. M.; Williams, L. R.; Wood, E. C.; Middlebrook, A. M.; Kolb, C. E.; Baltensperger, U.; Worsnop, D. R. Evolution of Organic Aerosols in the Atmosphere. *Science* **2009**, *326* (5959), 1525–1529. https://doi.org/10.1126/science.1180353.

(9) Shiraiwa, M.; Ammann, M.; Koop, T.; Pöschl, U. Gas Uptake and Chemical Aging of Semisolid Organic Aerosol Particles. *PNAS* **2011**, *108* (27), 11003–11008. https://doi.org/10.1073/pnas.1103045108.

(10) Koop, T.; Bookhold, J.; Shiraiwa, M.; Pöschl, U. Glass Transition and Phase State of Organic Compounds: Dependency on Molecular Properties and Implications for Secondary Organic Aerosols in the Atmosphere. *Phys. Chem. Chem. Phys.* **2011**, *13* (43), 19238–19255. https://doi.org/10.1039/C1CP22617G.

(11) Liu, C.-L.; Smith, J. D.; Che, D. L.; Ahmed, M.; Leone, S. R.; Wilson, K. R. The Direct Observation of Secondary Radical Chain Chemistry in the Heterogeneous Reaction of Chlorine Atoms with Submicron Squalane Droplets. *Phys. Chem. Chem. Phys.* **2011**, *13* (19), 8993. https://doi.org/10.1039/c1cp20236g.
(12) Lee, L.; Wilson, K. The Reactive–Diffusive Length of OH and Ozone in Model Organic Aerosols. *J. Phys. Chem. A* **2016**, *120* (34), 6800–6812. https://doi.org/10.1021/acs.jpca.6b05285.
(13) Davies, J. F.; Wilson, K. R. Nanoscale Interfacial Gradients Formed by the Reactive Uptake of OH Radicals onto Viscous Aerosol Surfaces. *Chem. Sci.* **2015**, *6* (12), 7020–7027. https://doi.org/10.1039/C5SC02326B.
(14) Houle, F. A.; Wiegel, A. A.; Wilson, K. R. Changes in Reactivity as Chemistry Becomes Confined to an Interface. The Case of Free Radical Oxidation of $C_{30}H_{62}$ Alkane by OH. *J. Phys. Chem. Lett.* **2018**, *9* (5), 1053–1057. https://doi.org/10.1021/acs.jpclett.8b00172.
(15) Richards-Henderson, N. K.; Goldstein, A. H.; Wilson, K. R. Large Enhancement in the Heterogeneous Oxidation Rate of Organic Aerosols by Hydroxyl Radicals in the Presence of Nitric Oxide. *J. Phys. Chem. Lett.* **2015**, *6* (22), 4451–4455. https://doi.org/10.1021/acs.jpclett.5b02121.
(16) Richards-Henderson, N. K.; Goldstein, A. H.; Wilson, K. R. Sulfur Dioxide Accelerates the Heterogeneous Oxidation Rate of Organic Aerosol by Hydroxyl Radicals. *Environ. Sci. Technol.* **2016**, *50* (7), 3554–3561. https://doi.org/10.1021/acs.est.5b05369.
(17) Zeng, M.; Liu, C.-L.; Wilson, K. R. Catalytic Coupling of Free Radical Oxidation and Electrophilic Chlorine Addition by Phase-Transfer Intermediates in Liquid Aerosols. *J. Phys. Chem. A* **2022**, *126* (19), 2959–2965. https://doi.org/10.1021/acs.jpca.2c00291.
(18) Zeng, M.; Heine, N.; Wilson, K. R. Evidence That Criegee Intermediates Drive Autoxidation in Unsaturated Lipids. *PNAS* **2020**. https://doi.org/10.1073/pnas.1920765117.
(19) Zeng, M.; Wilson, K. R. Efficient Coupling of Reaction Pathways of Criegee Intermediates and Free Radicals in the Heterogeneous Ozonolysis of Alkenes. *J. Phys. Chem. Lett.* **2020**, *11* (16), 6580–6585. https://doi.org/10.1021/acs.jpclett.0c01823.
(20) Reynolds, R.; Ahmed, M.; Wilson, K. R. Constraining the Reaction Rate of Criegee Intermediates with Carboxylic Acids during the Multiphase Ozonolysis of Aerosolized Alkenes. *ACS Earth Space Chem.* **2023**. https://doi.org/10.1021/acsearthspacechem.3c00026.
(21) Reid, J. P.; Bertram, A. K.; Topping, D. O.; Laskin, A.; Martin, S. T.; Petters, M. D.; Pope, F. D.; Rovelli, G. The Viscosity of Atmospherically Relevant Organic Particles. *Nature Communications* **2018**, *9* (1), 1–14. https://doi.org/10.1038/s41467-018-03027-z.
(22) Slade, J. H.; Knopf, D. A. Multiphase OH Oxidation Kinetics of Organic Aerosol: The Role of Particle Phase State and Relative Humidity. *Geophysical Research Letters* **2014**, *41* (14), 5297–5306. https://doi.org/10.1002/2014GL060582.
(23) Slade, J. H.; Ault, A. P.; Bui, A. T.; Ditto, J. C.; Lei, Z.; Bondy, A. L.; Olson, N. E.; Cook, R. D.; Desrochers, S. J.; Harvey, R. M.; Erickson, M. H.; Wallace, H. W.; Alvarez, S. L.; Flynn, J. H.; Boor, B. E.; Petrucci, G. A.; Gentner, D. R.; Griffin, R. J.; Shepson, P. B. Bouncier Particles at Night: Biogenic Secondary Organic Aerosol Chemistry and Sulfate Drive Diel Variations in the Aerosol Phase in a Mixed Forest. *Environ. Sci. Technol.* **2019**, *53* (9), 4977–4987. https://doi.org/10.1021/acs.est.8b07319.
(24) Denisov, E. T.; Afanas'ev, I. B. *Oxidation and Antioxidants in Organic Chemistry and Biology.*; Taylor & Frances: Oxford, 2005.

(25) Russell, G. A. Deuterium-Isotope Effects in the Autoxidation of Aralkyl Hydrocarbons. Mechanism of the Interaction of PEroxy Radicals1. *J. Am. Chem. Soc.* **1957**, *79* (14), 3871–3877. https://doi.org/10.1021/ja01571a068.
(26) Howard, J. A.; Ingold, K. U. Self-Reaction of Sec-Butylperoxy Radicals. Confirmation of the Russell Mechanism. *J. Am. Chem. Soc.* **1968**, *90* (4), 1056–1058. https://doi.org/10.1021/ja01006a037.
(27) Bennett, J. E.; Summers, R. Product Studies of the Mutual Termination Reactions of *Sec* -Alkylperoxy Radicals: Evidence for Non-Cyclic Termination. *Can. J. Chem.* **1974**, *52* (8), 1377–1379. https://doi.org/10.1139/v74-209.
(28) Docherty, K. S.; Ziemann, P. J. Reaction of Oleic Acid Particles with NO_3 Radicals: Products, Mechanism, and Implications for Radical-Initiated Organic Aerosol Oxidation. *J. Phys. Chem. A* **2006**, *110* (10), 3567–3577. https://doi.org/10.1021/jp0582383.
(29) George, I. J.; Abbatt, J. P. D. Heterogeneous Oxidation of Atmospheric Aerosol Particles by Gas-Phase Radicals. *Nature Chem* **2010**, *2* (9), 713–722. https://doi.org/10.1038/nchem.806.
(30) Zeng, M.; Liu, C.-L.; Wilson, K. R. Catalytic Coupling of Free Radical Oxidation and Electrophilic Chlorine Addition by Phase-Transfer Intermediates in Liquid Aerosols. *J. Phys. Chem. A* **2022**, *126* (19), 2959–2965. https://doi.org/10.1021/acs.jpca.2c00291.
(31) Zeng, M.; Wilson, K. R. Experimental Evidence That Halogen Bonding Catalyzes the Heterogeneous Chlorination of Alkenes in Submicron Liquid Droplets. *Chem. Sci.* **2021**, *12* (31), 10455–10466. https://doi.org/10.1039/D1SC02662C.
(32) Yin, H.; Xu, L.; Porter, N. A. Free Radical Lipid Peroxidation: Mechanisms and Analysis. *Chem. Rev.* **2011**, *111* (10), 5944–5972. https://doi.org/10.1021/cr200084z.
(33) Niki, E. Free Radical Initiators as Source of Water- or Lipid-Soluble Peroxyl Radicals. In *Methods in Enzymology*; Elsevier, 1990; Vol. 186, pp 100–108. https://doi.org/10.1016/0076-6879(90)86095-D.
(34) Heine, N.; Houle, F. A.; Wilson, K. R. Connecting the Elementary Reaction Pathways of Criegee Intermediates to the Chemical Erosion of Squalene Interfaces during Ozonolysis. *Environ. Sci. Technol.* **2017**, *51* (23), 13740–13748. https://doi.org/10.1021/acs.est.7b04197.
(35) Zhang, X.; Barraza, K. M.; Beauchamp, J. L. Cholesterol Provides Nonsacrificial Protection of Membrane Lipids from Chemical Damage at Air–Water Interface. *PNAS* **2018**, *115* (13), 3255–3260. https://doi.org/10.1073/pnas.1722323115.
(36) Wagner, J. P. Criegee Intermediates in Autoxidation Reactions: Mechanistic Considerations. *J. Phys. Chem. A* **2021**, *125* (1), 406–410. https://doi.org/10.1021/acs.jpca.0c09971.
(37) Chen, L.; Huang, Y.; Xue, Y.; Jia, Z. Molecular Insights into the Formation of Criegee Intermediates from β-Hydroxyperoxy Radicals. *Atmospheric Environment* **2024**, *338*, 120828. https://doi.org/10.1016/j.atmosenv.2024.120828.
(38) Zeng, M.; Wilson, K. R. Evaluating Possible Formation Mechanisms of Criegee Intermediates during the Heterogeneous Autoxidation of Squalene. *Environ. Sci. Technol.* **2024**, *58* (26), 11587–11595. https://doi.org/10.1021/acs.est.4c02590.
(39) Wells, J. R.; Morrison, G. C.; Coleman, B. K.; Spicer, C.; Dean, S. W. Kinetics and Reaction Products of Ozone and Surface-Bound Squalene. *J. ASTM Int.* **2008**, *5* (7), 101629. https://doi.org/10.1520/JAI101629.
(40) Berkemeier, T.; Mishra, A.; Mattei, C.; Huisman, A. J.; Krieger, U. K.; Pöschl, U. Ozonolysis of Oleic Acid Aerosol Revisited: Multiphase Chemical Kinetics and Reaction

Mechanisms. *ACS Earth Space Chem.* **2021**, *5* (12), 3313–3323. https://doi.org/10.1021/acsearthspacechem.1c00232.
(41) Taatjes, C. A. Criegee Intermediates: What Direct Production and Detection Can Teach Us About Reactions of Carbonyl Oxides. *Annu. Rev. Phys. Chem.* **2017**, *68* (1), 183–207. https://doi.org/10.1146/annurev-physchem-052516-050739.
(42) Welz, O.; Eskola, A. J.; Sheps, L.; Rotavera, B.; Savee, J. D.; Scheer, A. M.; Osborn, D. L.; Lowe, D.; Murray Booth, A.; Xiao, P.; Anwar H. Khan, M.; Percival, C. J.; Shallcross, D. E.; Taatjes, C. A. Rate Coefficients of C1 and C2 Criegee Intermediate Reactions with Formic and Acetic Acid Near the Collision Limit: Direct Kinetics Measurements and Atmospheric Implications. *Angewandte Chemie* **2014**, *126* (18), 4635–4638. https://doi.org/10.1002/ange.201400964.